Creep Fronts and Asperity Interactions in Laboratory Earthquake Sequences Illuminate Delayed Earthquake Triggering

Gregory C. McLaskey[1] (gcm8@cornell.edu), Sara Beth L. Cebry[1], Chun-Yu Ke[1], Srisharan Shreedharan[2,3], Chris Marone[2,4], David S. Kammer[5],

[1]School of Civil and Environmental Engineering, Cornell University, Ithaca, NY 14850, USA, [2]Dept. of Geosciences, Pennsylvania State University, University Park, PA 16802, USA, [3]University of Texas Institute for Geophysics, Austin, TX, [4]Dipartimento di Scienze della Terra, La Sapienza Università di Roma, Italy, [5]Institute for Building Materials, ETH, Zurich, Switzerland

1. Background and Motivation.

Seismic asperities are fault sections that are stronger and more seismogenic than their surroundings. Their properties may control earthquake size, and interaction between asperities is important for aftershocks, and earthquake triggering.

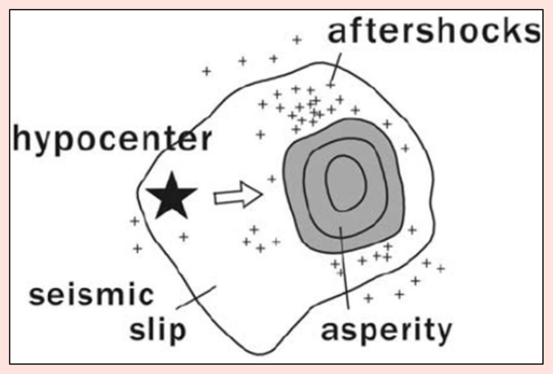

Yamanaka and Kikuchi, 2004

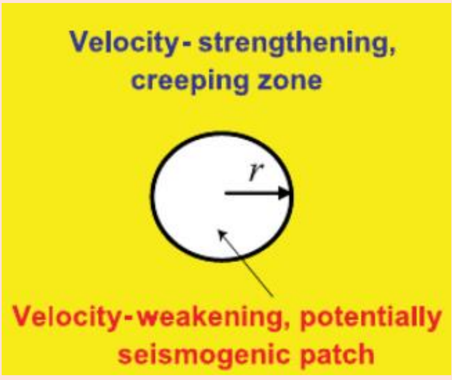

Chen and Lapusta, 2009

2. Laboratory Experiment with a Hybrid Sample.

Our sample has two dominant asperities: A1 (red) and A2 (blue) that result from locally high normal stress at the sample ends. A1 and A2 can rupture independently and interact through post-seismic slip in the form of creep fronts. We track slip with 8 slip sensors (color coded).

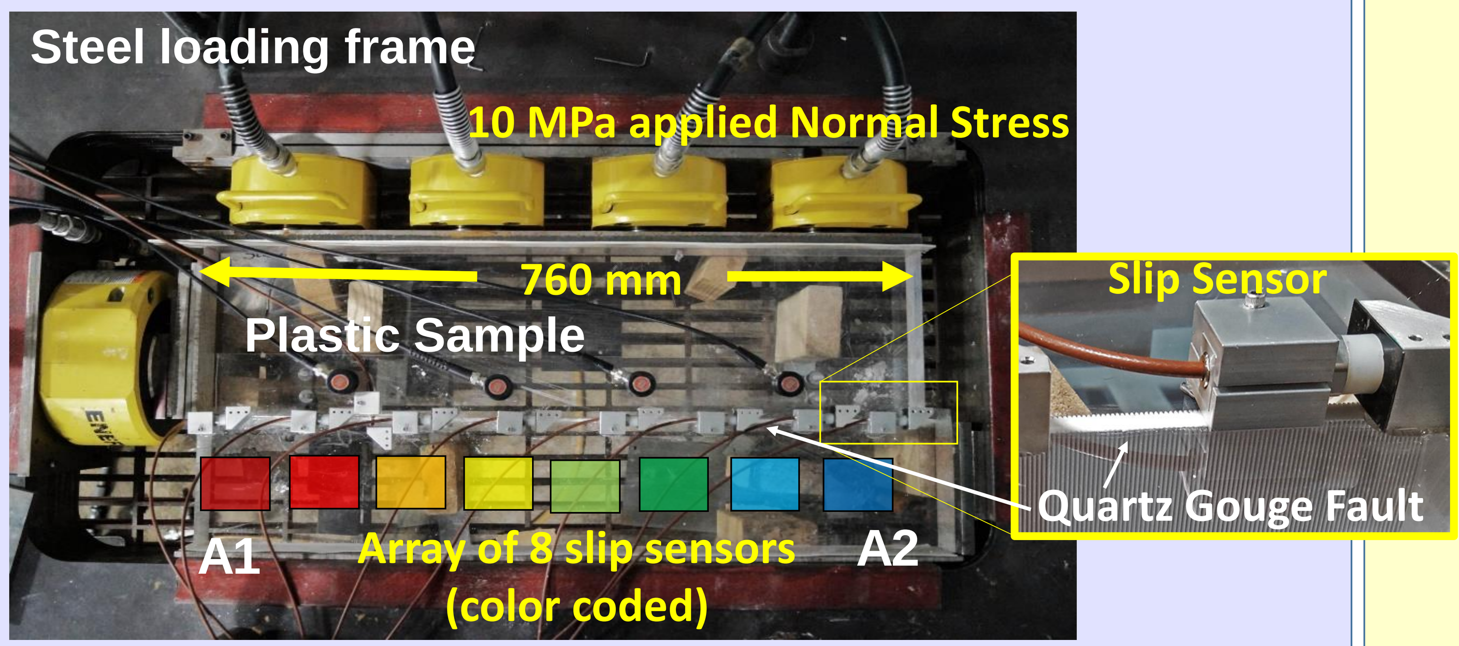

Using a recently-developed technique (Buijze et al., 2020), fault slip occurs within a 2 mm thick layer of powdered quartz (gouge) sandwiched between 760 mm-long plastic forcing blocks. Elastically, the plastic sample behaves like about 10 m of rock, but friction is controlled by the quartz gouge, and is well characterized by rate- and state-dependent friction. We use identical gouge layer preparation methods, so friction matches previous studies.

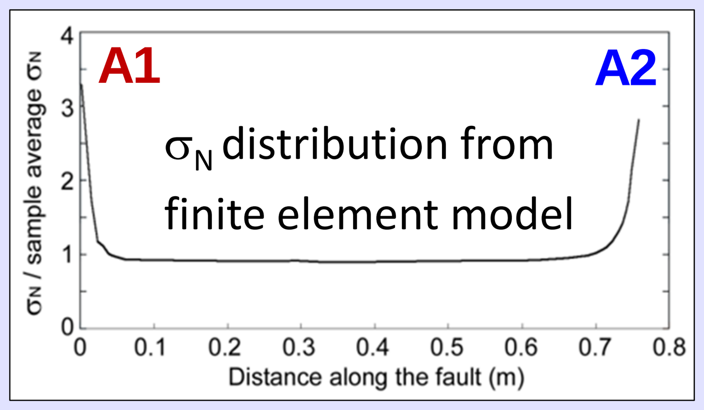

3. Previous quartz gouge research establishes friction evolution.

With continued shear strain, friction properties transition from velocity strengthening (b-a < 0) to velocity weakening (b-a > 0) while D_c decreases from 15 mm to 2-3 mm (the fault becomes more unstable). Friction evolution is well characterized with previous, smaller experiments shown below (Leeman et al., 2016; Scuderi et al., 2017). Those friction parameters are inputs for corresponding numerical models.

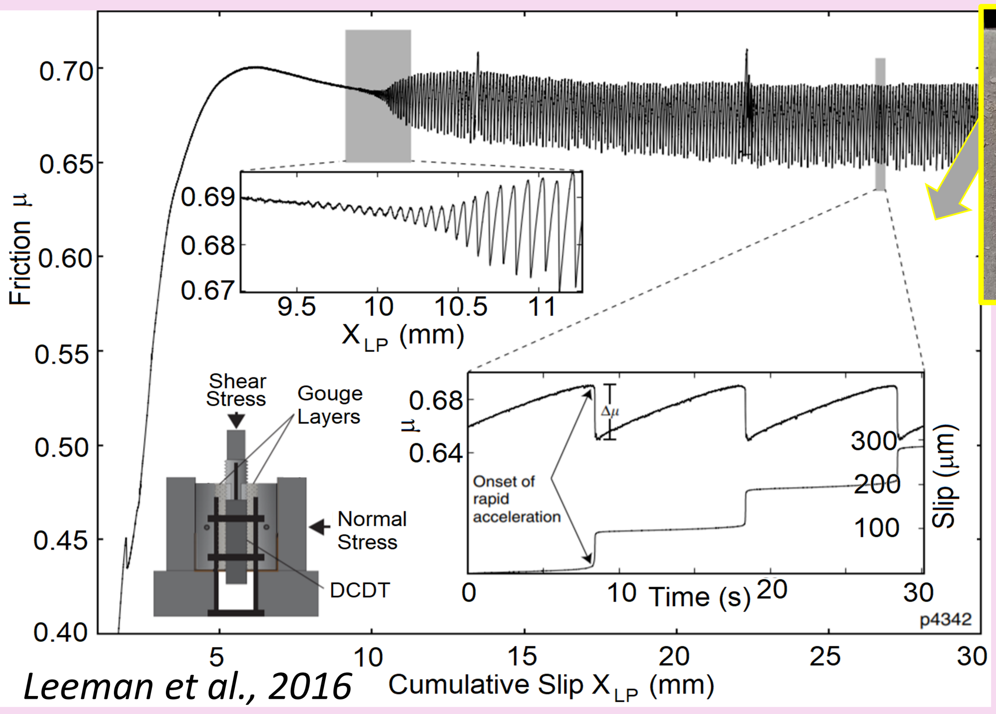

Leeman et al., 2016

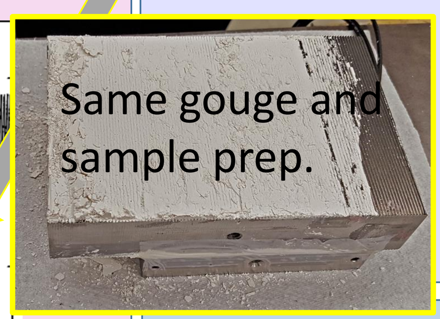

5. Mapping sample behavior in R_u – R_b space.

We map the previously established evolution of the friction parameters in R_u-R_b parameter space (gray arrow below). We then compare our sample behavior to that of the homogeneous model of Barbot (2019), shown below. Similar results were obtained by Cattania (2019).

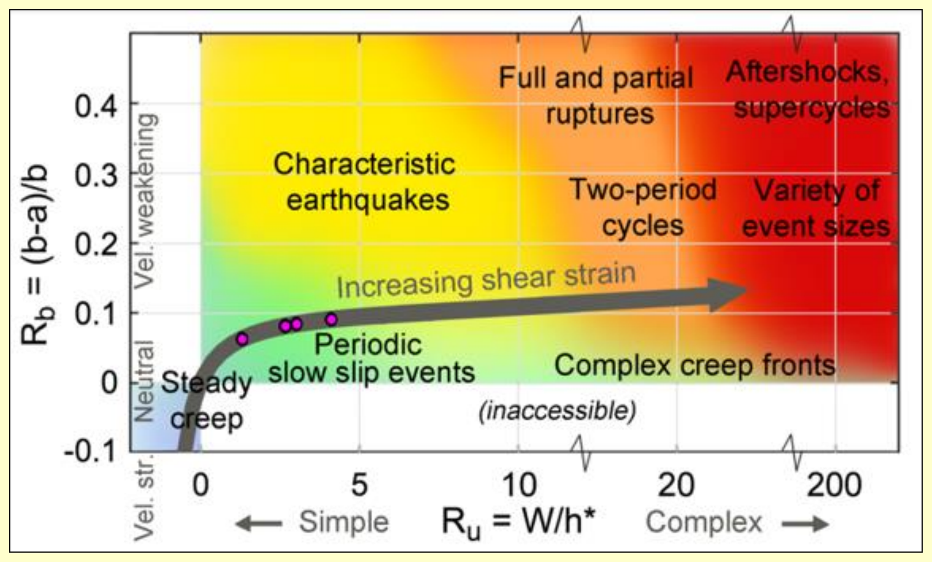

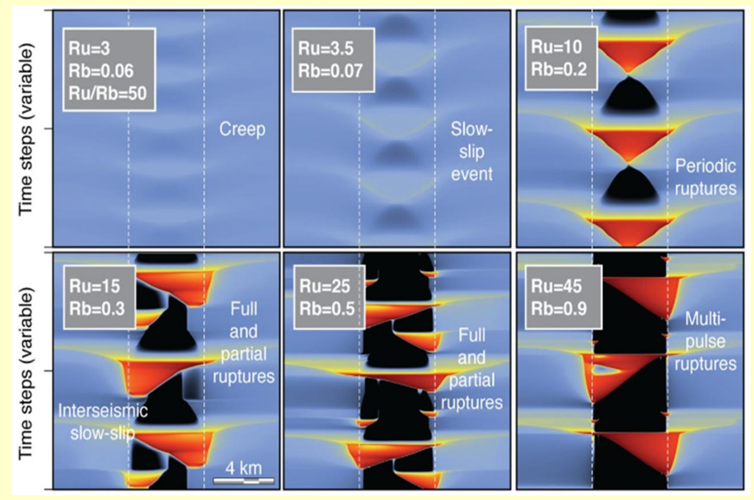

Barbot, 2019

R_u = W/h*, where W is the sample length, $h^* = 2D_cG'/(\pi\cdot\sigma_N(b-a))$ is a critical elasto-frictional length
R_b = (b-a)/b, which describes the intensity of frictional weakening behavior.

Slip independent Parameters		
sample length, W	0.76	m
normal stress, σ_N	10	MPa
shear modulus, G	1.1	GPa
Poisson's ratio, ν	0.35	
G' = G/(1-ν)	1.69	GPa

Our sample with two asperities produces a qualitatively similar behavioral progression to the homogeneous numerical simulations (Barbot, 2019; Cattania, 2019), but at lower R_u levels.

Slip Dependent Friction Parameters					
Cumulative slip, X_{LP} (mm)	5	10	15	20	25
shear strain	2	4	6	8	10
B	0.00726	0.01021	0.01125	0.01179	0.01213
D_c (μm)	11.266	5.0766	3.1847	2.2876	1.7699
b-a	-0.00081	0.00044	0.00082	0.00101	0.00114
a	0.00807	0.00977	0.01043	0.01078	0.01099

Slip Dependent Friction Parameters						
Cumulative slip, X_{LP} (mm)		5	10	15	20	25
$h^* = 2D_cG'/(\pi\sigma_N(b\text{-}a))$	(m)	-1.507	1.239	0.416	0.243	0.167
$L_b = D_cG'/(\sigma_N b)$	(m)	0.263	0.084	0.048	0.033	0.025
W / h*		-0.50	0.61	1.83	3.13	4.54
$L/L_b = W/2/L_b$		1.45	4.52	7.93	11.57	15.39

4a. Sample Behavior Evolves From Simple to Complex.

We apply constant normal stress and slowly shear the sample at 6 μm/s. Over many mm of cumulative slip, steady sliding gives way to slow slip events (A), characteristic stick-slip events, two-period cycles (B), and then a variety of event sizes (C).

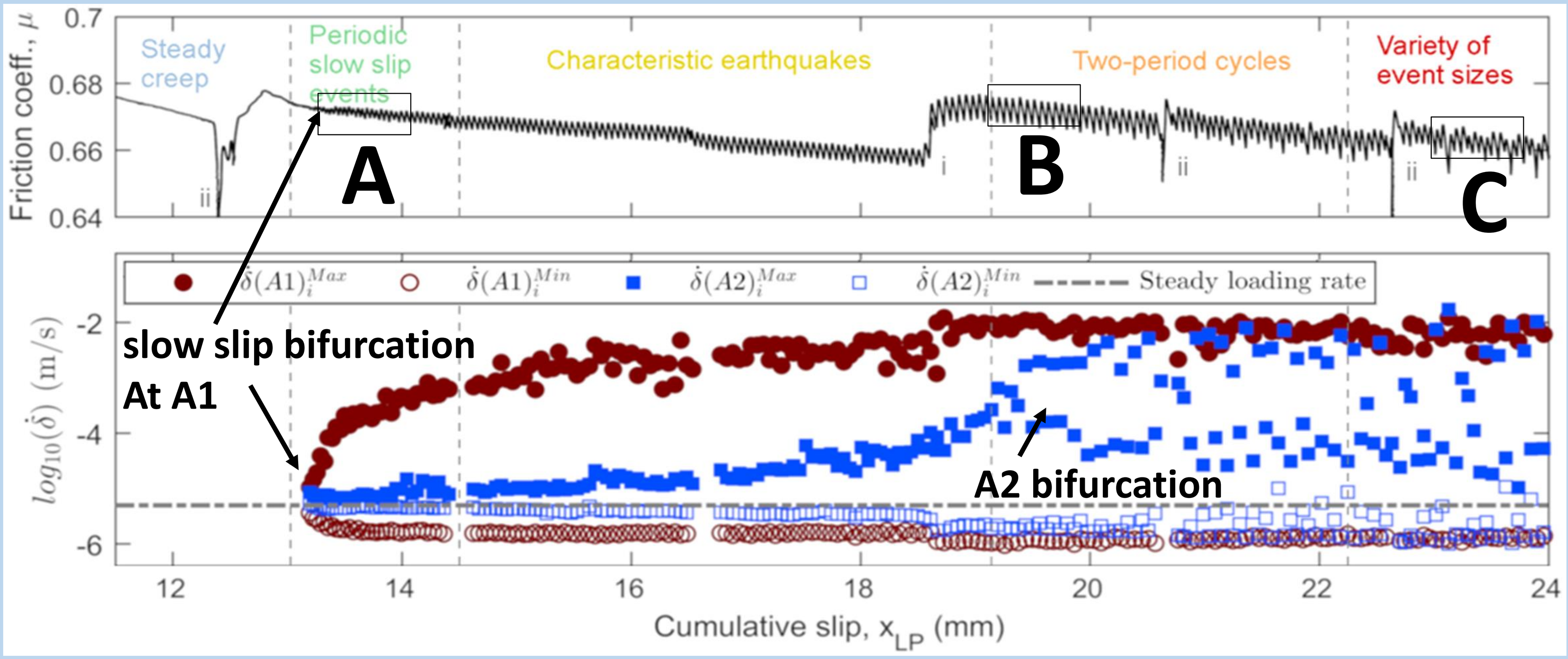

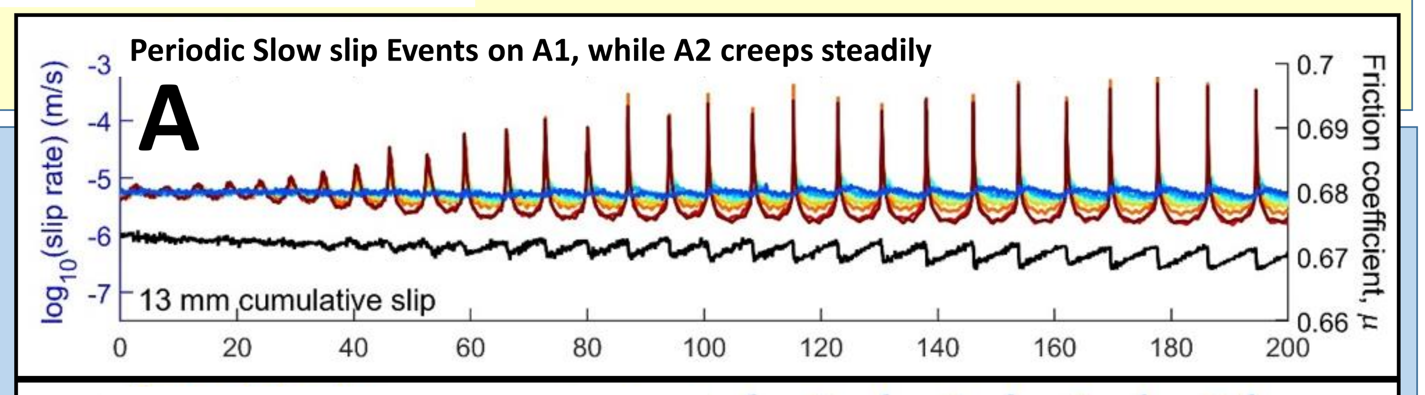

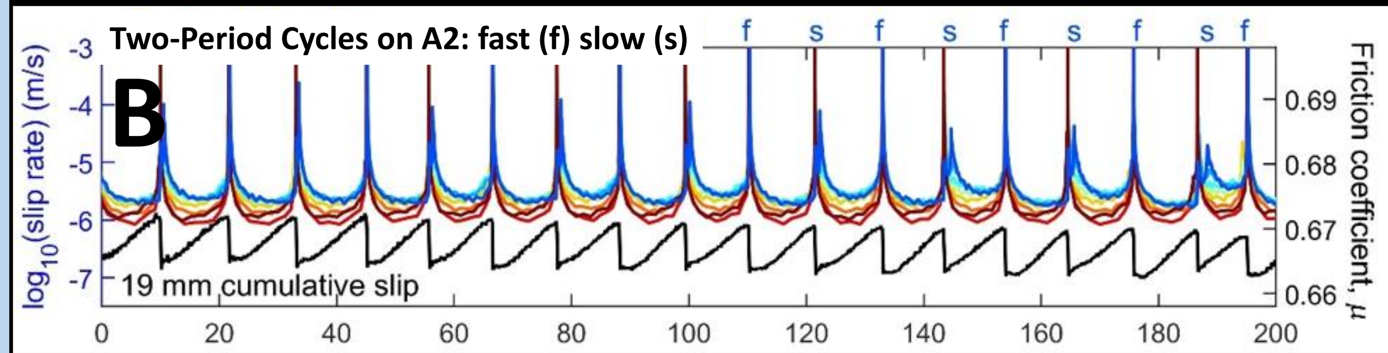

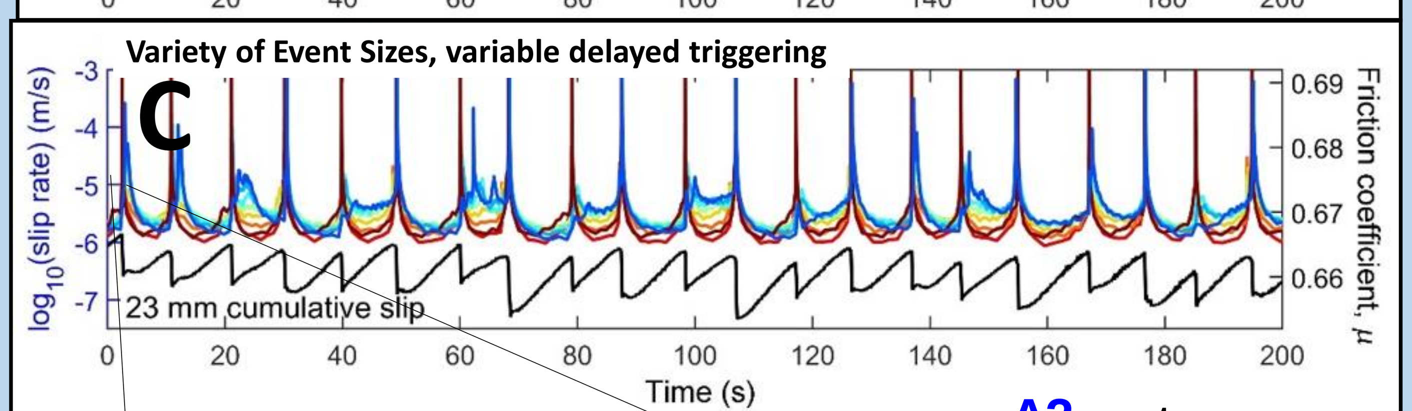

6. Numerical Models:

We simulate the 2-asperity interactions with fully dynamic, 2D spectral boundary integral method. With constant friction properties along the sample, the two asperities are regions with locally high shear stress. The size and stress state of the asperities were first tuned to yield spontaneous rupture of A1 followed by delayed rupture of A2. Then, keeping stress levels at A1 and A2 constant, we studied the triggering behavior as a function of the shear stress level (τ_0) between the two asperities and changing friction parameters. We model shear stress asperities instead of normal stress asperities. This only works because they are single-cycle simulations (asperities rupture only once).

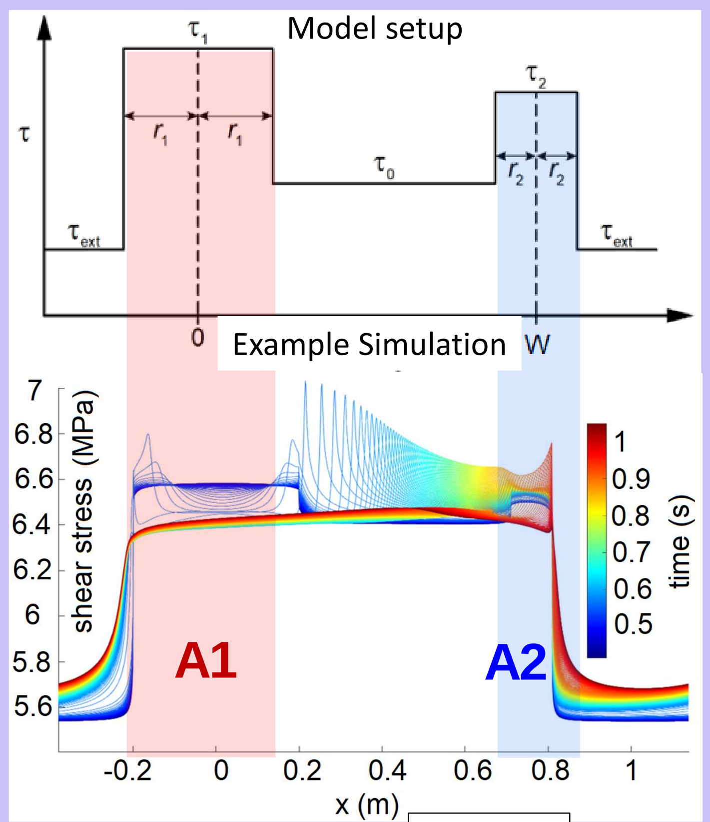

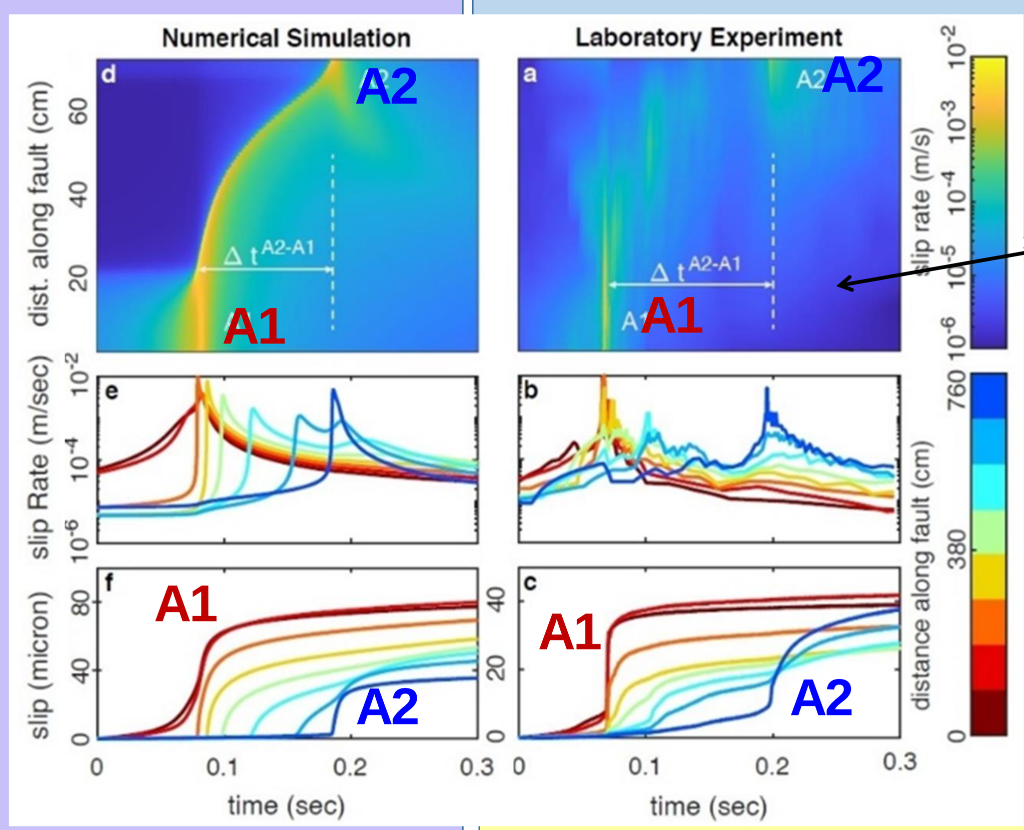

4b. Creep Fronts Propagate Between the Asperities.

The figures on the left and right show zoom-ins of local slip measurements and corresponding slip rate maps showing rupture of one asperity, propagation of a creep front, and subsequent rupture of another asperity. Typically, A1 ruptures first (left), but sometimes it's reversed (right).

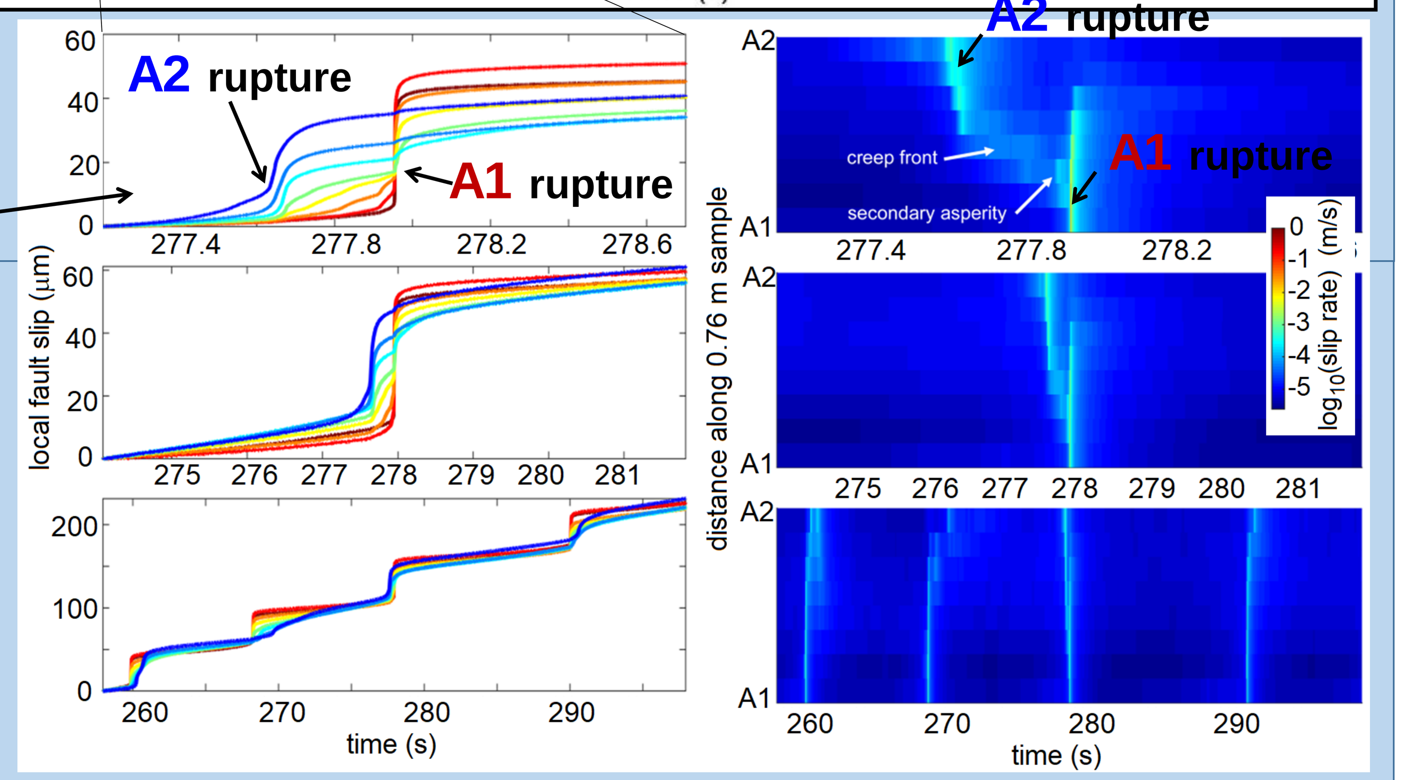

7. Conclusions:

The simulations show that small changes in initial shear stress τ_0 (50 kPa) cause two orders of magnitude variation in the average triggering speed of the creep fronts. Fronts propagate faster at higher τ_0, consistent with other recent studies (Garagash, 2021). Using strain gages, we find a similar stress dependence in our experiments: 20 kPa variation in initial overstress τ_0 can cause an order of magnitude change in A1-to-A2 triggering velocity.

The sensitivity to τ_0 explains the oscillatory behavior of the A2 bifurcation observed at x_{LP} = 19 mm: stronger A2 events reduced stress levels in the region surrounding A2 more significantly so the subsequent creep front propagates slowly and triggers weaker A2 events. Weaker A2 events have smaller stress drop and thus do not reduce stress levels as much, which primes the fault for faster subsequent creep fronts and more rapid triggering of stronger events.

With evolving friction (increased R_u and increased creep propagation distance L/L_b), creep front behavior becomes less sensitive to the size of the events that initiate them (hypocentral forcing) and increasingly sensitive to small variations in initial overstress levels (Garagash 2021). This is the likely reason for the increasingly complex behavior observed late in the experiment, despite highly periodic behavior early on.

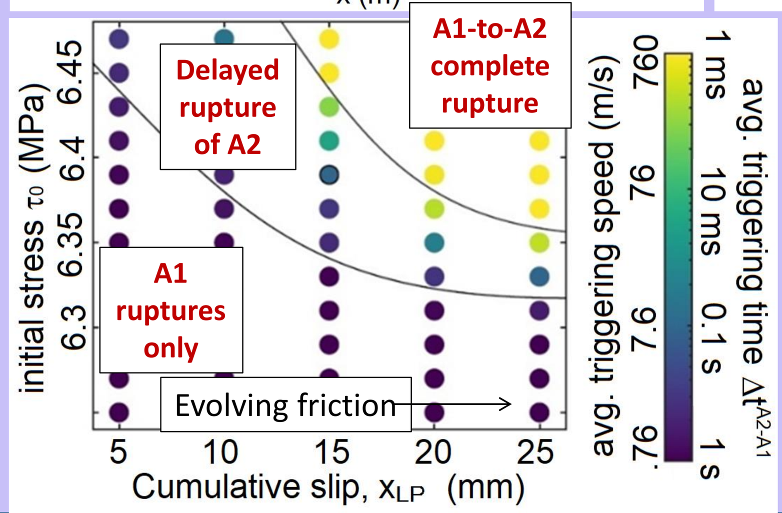

At left: results of a suite of simulations. Each circle is a simulation, color-coded by the A1-to-A2 triggering time. With more slip, the triggering time is more sensitive to τ_0.

Acknowledgements: A. Zhang, K. Sorhaindo, and T. Brock assisted with sample preparation. Comments from three anonymous reviewers improved the study. We gratefully acknowledge NSF grants EAR-1763499, EAR-1847139, and EAR-1763305.

References:
1. Barbot, S. (2019) Slow-slip, slow earthquakes, period-two cycles, full and partial ruptures, and deterministic chaos in a single asperity fault. *Tectonophysics* **768**, 228171.
2. Buijze, L., Guo, Y., Niemeijer, A. R., Ma, S. & Spiers, C. J. (2020) Nucleation of Stick-Slip Instability… Stress Heterogeneities Due to Loading and Gouge Layer Compaction. *J. Geophys. Res. Solid Earth* **125**, e2019JB018429.
3. Cattania, C. (2019) Complex Earthquake Sequences On Simple Faults. *Geophys. Res. Lett.* **46**, 10384–10393.
4. Chen, T., and N. Lapusta (2009), Scaling of small repeating earthquakes explained by interaction of seismic and aseismic slip in a rate and state fault model, J. Geophys. Res. Solid Earth, 114, B01311.
5. Garagash, D. I. (2021) Fracture mechanics of rate-and-state faults and fluid injection induced slip. *Philos. Trans. R. Soc. Math. Phys. Eng. Sci.* **379**, 20200129.
6. Leeman, J. R., Saffer, D. M., Scuderi, M. M. & Marone, C. (2016) Laboratory observations of slow earthquakes and the spectrum of tectonic fault slip modes. *Nat. Commun.* **7**, 11104.
7. Scuderi, M. M., Collettini, C., Viti, C., Tinti, E. & Marone, C. (2017) Evolution of shear fabric in granular fault gouge from stable sliding to stick slip and implications for fault slip mode. *Geology* **45**, 731–734.
8. Yamanaka, Y., and M. Kikuchi (2004), Asperity map along the subduction zone in northeastern Japan inferred from regional seismic data, J. Geophys. Res., 109, B07307.